International Journal of Power Electronics and Drive System (IJPEDS)
Vol. 6, No. 2, June 2015, pp. 293~304
ISSN: 2088-8694

Open-Switch Fault-Tolerant Control of a Grid-Side Converter in a Wind Power Generation System

Partha Sarati Das, Kyeong-Hwa Kim
Departement of Electrical and Information Engineering
Seoul National University of Science and Technology, Seoul, Korea

Article Info

Article history:

Received Jan 14, 2015
Revised Apr 28, 2015
Accepted May 12, 2015

Keyword:

Fault-tolerant
Grid-side converter
Machine-side converter
Open-switch fault
Wind energy conversion system

ABSTRACT

A fault-tolerant technique of a grid-side converter (GSC) is a very important task because the unbalanced grid power endangers the overall system. Since the GSC is very sensitive to grid disturbance, the complete system needs to be stopped suddenly once an open-switch fault occurs. To improve the reliability of system, the continuous operation should be guaranteed. In this paper, a redundant topology based fault-tolerant algorithm is proposed for a GSC in a wind power generation system. The proposed scheme consists of the fault detection and fault-tolerant algorithms. The fault detection algorithm employs the durations of positive and negaitive cycles of three-phase grid currents as well as normalized root mean square (RMS) currents. Once a fault is detected, the corresponding faulty phase is identified and isolated to enable the fault-tolerant operation. The faulty phase is replaced by redundant one rapidly to recover the original shape of the grid currents, which ensures the continuity in operation. In contrast with the conventional methods, the proposed fault detection and fault-tolerant algorithms work effectively even in the presence of the open faults in multiple switches in the GSC. Simulation results verify the effectiveness of the proposed fault diagnosis and fault-tolerant control algorithms.

Corresponding Author:

Kyeong-Hwa Kim,
Departement of Electrical and Information Engineering,
Seoul National University of Science and Technology,
232 Gongneung-ro, Nowon-gu, Seoul, 139-743, Korea.
Email: k2h1@seoultech.ac.kr

1. INTRODUCTION

Wind, solar, and biomass are renewable energy sources that replace conventional fuels such as oil or natural gas. The efficiency and performance of renewable energy systems are still under development. Most of renewable energy technologies are used in grid connected power generation system. The control structures of the grid connected converter are a vital portion for energy conversion and transmission which needs to be improved to meet the requirements for grid interconnection. A grid-side converter (GSC) converts the DC electric energy from the renewable energy source into AC electric energy, which transfers the DC link power to grid.

Wind energy is becoming more and more important to reduce reliance on fossil fuel, which leads to a variety of research and development of wind power generation technology. There are two types of inverter scheme depending on its operation, that is the stand-alone inverter and grid connected inverter. The GSC for wind turbine converts DC power produced by a wind turbine generator to AC power to supply electrical load or transfer the excessive power to utility grid. In this case, the inverter output voltage and frequency should be same as those of the grid. In the grid connected inverter, output should be synchronized with the grid to meet the requirements in grid interconnection.

The issue on the reliability, continuity, and fault has received intensive research interests in the development of electrical power systems. A fault in the power system produces the safety problem as well as the increased loss due to shutdown of system. Thus, the correct diagnosis and remedial strategy through the early detection of faults are important to avoid harmful accidents and to guarantee a continuity of operation. Furthermore, power system downtime for unscheduled maintenance can be minimized, which results in less economical losses. For this reason, many research works have been investigated in electric power systems or power electronics equipments.

Two different types of fault-tolerant pulse width modulated (PWM) inverter-fed AC motor drive system have been proposed in to determine the faulty device in PWM voltage source inverter drives for open-switch and short-switch failures [1]. In this scheme, the expenditure in two fault-tolerant configurations was demonstrated and experimental results have been presented to prove the successful fault compensation. A fuzzy logic based fault diagnosis method for three parallel converters in a wind turbine system was studied [2]. This method can not only detect both open-switch and short-switch faults but can also identify faulty switching devices without additional voltage sensor or an analytical system model. Open-switch and short-switch faults can be detected by analyzing the stator current patterns within the maximum of two current periods. The location of a faulty switch can be indicated by six patterns of a stator current vector and the faulty switching device is detected by analyzing the current vector. A diagnostic algorithm that allows the real-time detection and localization of multiple open-switch faults in inverter-fed AC motor drives has been presented [3]. This method is quite simple and just requires the measured motor phase currents and their corresponding reference signals, which are already available from the main control system. Moreover, this algorithm does not depend on the motor power, load, and speed. For a PWM voltage source inverter based induction motor drive, fault detection and diagnosis schemes have been studied using the fuzzy logic [4]. This work requires the measurement of the output inverter currents to detect the intermittent loss of firing pulses in inverter power switches. Fault-tolerant strategies for neutral point clamped (NPC) inverter systems feeding high power induction motor drives have been proposed with very low cost [5]. Two different fault converter strategies have been compared with the use of additional components. A comparative literature review on the existing methods was discussed for fault diagnosis and protection including open-switch, short-switch, and gate misfiring faults in three-phase power inverters [6]. Twenty-one methods for open-switch faults and ten methods for short-switch faults were evaluated and summarized based on their performance and implementation efforts. The gate-misfiring faults and corresponding diagnostic methods have also been discussed briefly.

A three-phase FPGA-based fault-tolerant back-to-back converter was proposed with a very fast fault detection scheme [7]. The fault-tolerant converter works like a conventional back-to-back six-leg converter before the fault occurrence and it works as a five-leg converter after the fault occurrence. Design, implementation, and experimental verification of a FPGA-based reconfigurable control strategy were discussed for this converter. For a voltage source inverter feeding AC machines, a real-time diagnostic scheme has been reported to detect the open fault in multiple switches [8]. In contrast with the majority of methods, only three-phase motor currents are used, which are already available for the main control system, avoiding the use of extra sensors. This method can handle large transients such as load and speed variations. A two-level fault-tolerant voltage source inverter for permanent magnet drive has been proposed [9], which provides tolerance to both short-switch and open-switch faults of the switching devices. Experimental results show that the compensation strategy is fast enough and the thyristors can successfully isolate the faulty leg in all the fault cases.

Fault-tolerant operation is very important for high impact automotive applications such as electrical vehicles and hybrid electrical vehicles. An active fault-tolerant control system has been presented for a high performance induction motor drive that propels an electrical vehicle or a hybrid electrical vehicle [10]. A fault-tolerant control system which can change the control technique in the event of sensor failures has been reported for an induction motor drive [11], where four control schemes have been used to ensure the continuity in motor drive operation. A fault-tolerant powertrain for series hybrid electric vehicles with two different techniques has been studied [12]. The time-domain simulation and experimental results evidently proved that these techniques work well in short-switch and open-switch fault. A modular power electronic converter with a cascaded H-bridge multilevel inverter has been proposed [13]. Several fault detection methods were analyzed, and one was tested based on monitoring the DC link voltage.

A fault-tolerant scheme for a doubly-fed induction generator (DFIG) wind turbine was presented using a parallel grid side rectifier and series GSC [14]. A fault-tolerant control has been proposed for a battery energy storage system based on a cascade PWM converter with star configuration [15]. Open-switch fault detection and replacement of the faulty switches have been proposed [16]. The detection of faulty switches was done by measuring the phase and line voltages of inverter. The replacement of faulty switch was done by using the extra arm. Performance analysis of three-phase induction motor drive system under open-switch fault has been discussed [17], where the open-switch fault was investigated at normal operating condition as well as faulty condition. During the occurrence of a single-converter-cell or single-battery-unit fault, the fault-tolerant control enables continuous operation which enhances system reliability and availability.

Without proper fault detection and fault-tolerant operation, the overall system has to be stopped suddenly under the open-switch fault in a wind power generation system. This is not acceptable because the system downtime due to the unscheduled maintenance or shutdown may decrease the system performance as well as the reliability and consistency of system. It is very important to make reliable detection and fault-tolerant algorithms because the system restoration can be accomplished quickly. From the studies investigated above, it can be observed that the detection, isolation, and reconfiguration techniques of open-switch fault in a grid connected converter for wind power generation system are not sufficient for improving the reliability. Therefore, more research works need to be done, which is a challenging task for researcher.

This paper proposes fault-tolerant compensation approaches for a GSC in wind power generation system. The total configuration consists of the machine-side converter (MSC) and GSC in a back-to-back topology, where the GSC has three additional inverter legs to beused as redundant hardware system. The open-switch fault is detected by using the normalized RMS currents. The proposed fault-tolerant strategy uses the information on the durations of positive and negative cycles in grid currents to find the location of open-switch fault. Once the location of open-switch fault is obtained, the fault-tolerant algorithm makes the system keep running with good performance. The proposed method does not need any additional current sensor because it uses only the durations of three-phase grid currents. Three current sensors are used to control the inverter. The proposed method is simple enough to be implemented in grid side controller, which allows the continuous operation of energy transfer to grid even in the presence of complete loss in multiple inverter legs.

2. FAULT-TOLERANT CONTROL OF GSC IN WIND ENERGY CONVERSION

Figure 1 shows the proposed fault-tolerant wind energy conversion system (WECS) topology, which is based on a classical back-to-back converter and uses common redundant legs for the GSC. The proposed fault-tolerant system is composed of three different units which are the phase isolation unit, phase reconnection unit, and additional leg unit. The redundant legs consist of the switches S_7, S_8, S_9, S_{10}, S_{11}, and S_{12}, and are used to replace the faulty one of the other legs under any power switch failure in the GSC. The redundant legs are not used normally when the GSC works without any fault.

Phase isolation unit uses three triode for alternating current (TRIAC) switches, which is located between the output terminals of the GSC and the corresponding phases in grid. These TRIAC switches are used to isolate the switches in faulty leg. The reconnection unit which also consists of three TRIAC switches is located between the output terminals of the redundant legs and the corresponding phases in grid as shown in Figure 1. These TRIAC switches are used in order to insert the redundant leg in place of the faulty phase. During the normal operation, three TRIAC switches in the isolation unit are turned ON whereas three TRIAC switches in the reconnection unit are turned OFF.

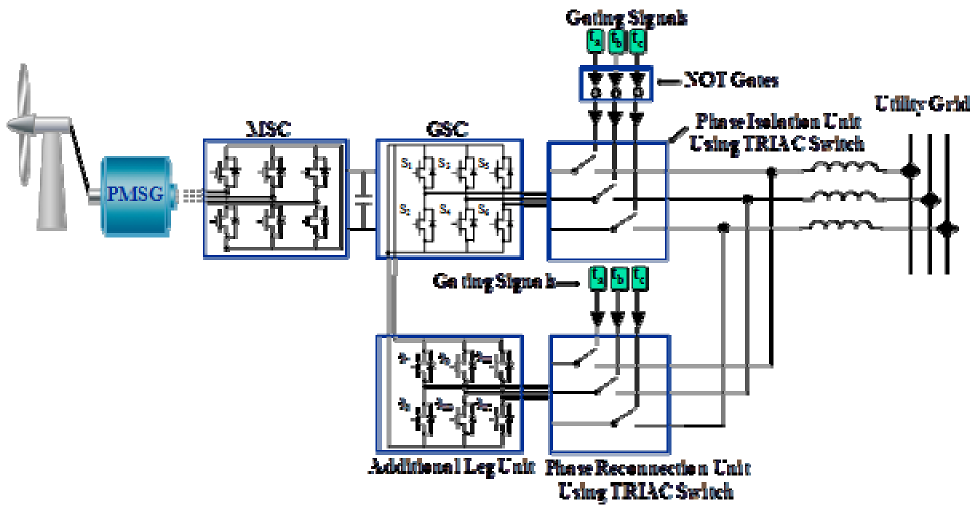

Figure 1. Proposed fault-tolerant scheme of GSC in WECS topology

Figure 2 shows the operation of the entire system during the normal healthy operation. During healthy operation, the additional leg unit will be inactive. However, as soon as the fault detection algorithm detects the open fault in the GSC, the faulty phase will be isolated. By using the gating signal, the isolated faulty phase is replaced with the additional leg unit to allow continuous operation of the GSC. The switching patterns are determined by gating signal.

An open-switch fault in the insulated gate bipolar transistor (IGBT) may occur due to the failure in the gate drive circuit or the break of bond wires in the IGBT. When one of the IGBTs cannot be turned ON, the corresponding phase current is zero during a half cycle, either positive or negative half cycle depending on the position of the IGBT switch. As a result, DC current offset is induced in the faulty phase and this offset is uniformly divided between the healthy phases. As soon as the open-switch fault in any IGBT is detected, the gating signal in faulty phase is stopped in the GSC and applied to the redundant leg in additional unit. At the same time, the TRIAC switch of the isolation unit is turned OFF to isolate the faulty leg and the TRIAC switch of the reconnecetion unit is turned ON.

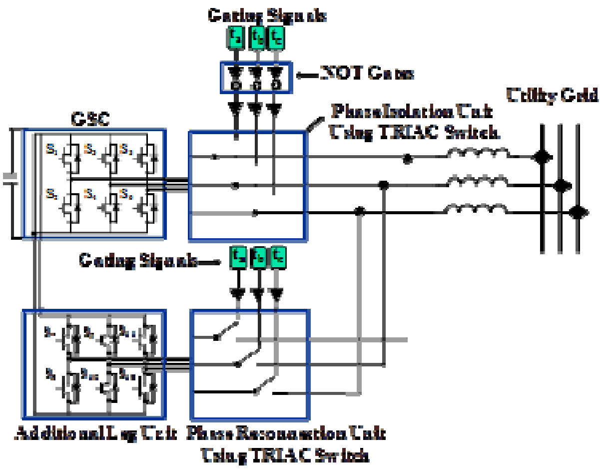

Figure 2. Fault-tolerant topology during normal operation

Figure 3 shows the fault-tolerant topology under the switch S_1 open fault. When the fault is introduced into system, the proposed detection algoritm effectively finds out the fault occurrence as well as its location. As soon as the fault location is determined, a remedial strategy is performed to guarantee a continuity of operation. In this case, *a*-phase TRIAC of the isolation unit is turned OFF and *a*-phase TRIAC of the reconnection unit is turned ON at the same time.

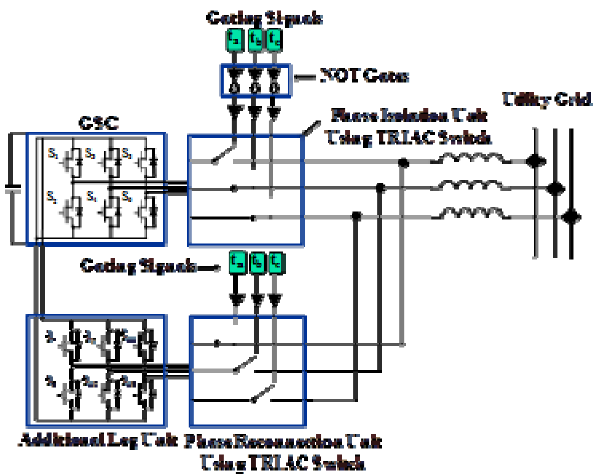

Figure 3. Fault-tolerant topology under the switch S_1 open fault

Figure 4 shows the fault-tolerant topology under the switches S_1 and S_3 open fault. Because the faults occur in *a*-phase and *b*-phase simultaneously, *a*-phase and *b*-phase TRIAC switches of the isolation unit are turned OFF and *a*-phase and *b*-phase TRIAC switches of the reconnection unit are turned ON. The gating signals of t_a, t_b, and t_c are utilized to turn ON and OFF the TRIAC switches, if any open-switch fault occurs. These gating signals are determined using the durations of corresponding phase current. During the normal operation, the values of t_a, t_b, and t_c used for the gating signals are zero to turn ON the TRIAC switches in the isolation unit. Under the fault condition, on the contrary, these values are changed to one to turn OFF the TRIAC switches in the isolation unit and to turn ON the TRIAC switches in the reconnection unit simultaneously.

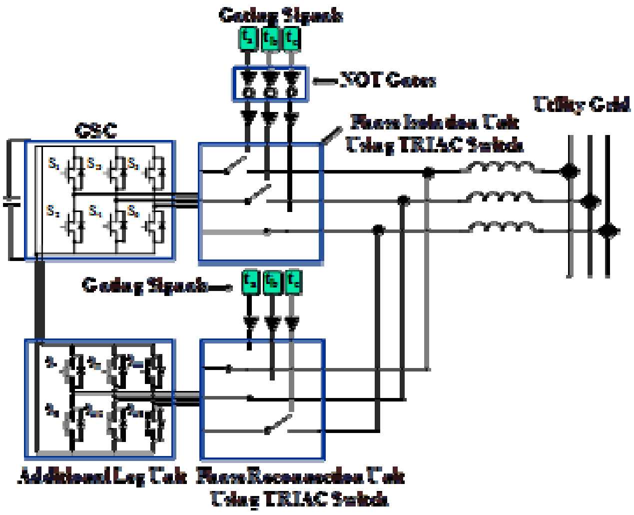

Figure 4. Fault-tolerant topology under the switches S_1 and S_3 open fault

3. PROPOSED FAULT DETECTION AND TOLERANT ALGORITHMS

The voltage model of three-phase MSC with a permanent magnet synchronous generator (PMSG) in the synchronous reference frame is given as follows:

$$e_{qm} = R_s i_{qm} + L_q \frac{di_{qm}}{dt} + \omega_e L_d i_{dm} + v_{qm} \tag{1}$$

$$e_{dm} = R_s i_{dm} + L_d \frac{di_{dm}}{dt} - \omega_e L_q i_{qm} + v_{dm} \tag{2}$$

where the subscript "m" denotes the variables in the MSC, e_{qm} and e_{dm} are the *q*-axis and *d*-axis generated voltages, respectively, i_{qm} and i_{dm} are the *q*-axis and *d*-axis generated currents, respectively, R_s is the stator resistance, L_q and L_d are the *q*-axis and *d*-axis inductances, respectively, ω_e is the electrical angular velocity of the generator. If the PMSG is a surface mounted type, then the *d*-axis and *q*-axis inductance are the same which is referred as no saliency. When the generated voltage is aligned to the *q*-axis in the synchronous reference frame, the generated voltages by the PMSG are obtained as follows:

$$e_{qm} = E = \omega_e \lambda_m \tag{3}$$

$$e_{dm} = 0 \tag{4}$$

where λ_m is the flux linkages. By controlling the DC link voltage constantly, the GSC can deliver the generated power from the MSC to grid. The converter input power can be expressed in terms of *d*-axis and *q*-axis variables in (2) as follows:

$$P_{in} = \frac{3}{2}(e_{dm}i_{dm} + e_{qm}i_{qm}) = \frac{3}{2}Ei_{qm} \quad (5)$$

If the loss in converter input resistor and inductor is neglected, the input power P_{in} is equal to that of converter output P_o. Thus, the converter output power can be expressed as

$$P_o = V_{dc}i_o \quad (6)$$

where V_{dc} is the DC link voltage and i_o is the converter output current.

A flow chart of the proposed fault detection and fault-tolerant algorithms is presented in Figure 5.

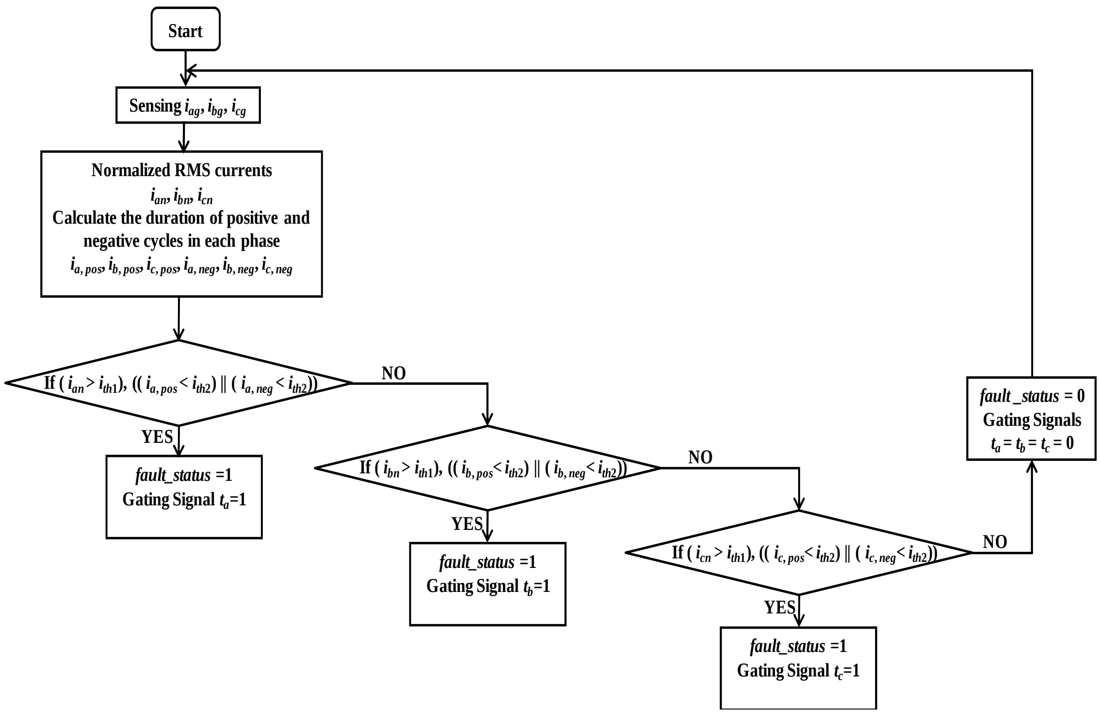

Figure 5. Flow chart of the proposed open-switch fault detection and fault-tolerant algorithm

Three-phase grid currents are transformed into the values on the stationary reference frame as follows:

$$i_{dg} = \frac{2}{3}i_{ag} - \frac{1}{3}i_{bg} - \frac{1}{3}i_{cg} \quad (7)$$

$$i_{qg} = \frac{1}{\sqrt{3}}(i_{bg} - i_{cg}) \quad (8)$$

where the subscript "g" denotes the variables in the GSC, and i_{ag}, i_{bg}, and i_{cg} are the three-phase grid currents, respectively. Using these values, the Park's vector modulus i_{sm} is obtained by

$$i_{sm} = \sqrt{i_{dg}^2 + i_{qg}^2}\ . \quad (9)$$

Three-phase RMS grid currents are normalized by using this Park's vector modulus as follows:

$$i_{an} = \frac{i_{arms}}{i_{sm}} \quad (10)$$

$$i_{bn} = \frac{i_{brms}}{i_{sm}} \tag{11}$$

$$i_{cn} = \frac{i_{crms}}{i_{sm}} \tag{12}$$

where i_{arms}, i_{brms}, and i_{crms} are three-phase RMS grid currents, respectively, and i_{an}, i_{bn}, and i_{cn} are the normalized three-phase RMS grid currents, respectively.

In the proposed fault detection algorithm, three-phase grid currents i_{ag}, i_{bg}, and i_{cg} are sensed at first by using the current sensor. From these values, the normalized three-phase RMS grid currents are calculated by using three-phase RMS grid currents and Park's vector modulus. The durations of positive and negative cycles in each phase currents are calculated from the current measurements. Open-switch fault detection is acheived by using the normalized three-phase RMS grid currents. Once the fault is detected, the faulty switch identification algorithm finds the location of faulty switch by using the durations of positive and negative cycles as the identification variables.

Under the normal operating condition, the normalized RMS current values become 0.5. On the other hand, these values are significantly increased for the open-switch fault condition. For the fault detection, the threshold value for the normalized RMS current is chosen as i_{th1}= 5.0. When an open-switch fault is introduced in any combination of switch, one of three detection variables which are i_{an}, i_{bn}, and i_{cn} is increased. To make sure of fault occurrence, the controller judges the fault event when one of these values is larger than the threshold value i_{th1}.

Fault-tolerant algorithm is activated once the fault is detected. After the fault detection, a reconfiguration is required in hardware as well as in software. Hardware reconfiguration is done by replacing the faulty phase with redundant one. In software part, the isolation and reconnection signals are generated as soon as the faulty switch is identified.

The durations of positive and negative cycle are used to trigger the gating signal of the TRIAC switches. Because the durations of positive and negaitive cycles in three-phase grid currents are varied due to the open-switch fault location, they can be utilized in order to find out the faulty phase. For example, if the open-switch fault occurs in S_1 as shown in Figure 1, a-phase current has only the duration of negative cycle because the faulty switch S_1 can not conduct any current. To distinguish the faulty phase, $i_{a,pos}$, $i_{b,pos}$, $i_{c,pos}$, $i_{a,neg}$, $i_{b,neg}$, and $i_{c,neg}$ are obtained from three-phase grid currents, which are used as faulty phase identification variables. By comparing these faulty phase identification variables with the threshold value i_{th2}, the faulty phase can be identified and the gating signals t_a, t_b, and t_c can be determined as shown in Figure 5. To find out the faulty phase instantly, the threshold value of i_{th2} is chosen as 4.0. The determined gating signals are used to trigger the TRIAC switches of two different set, that is, the phase isolation unit and the phase reconnection unit in Figure 1 for fault-tolerant compensation.

4. SIMULATION RESULTS

The effectiveness of the fault detection, identification, and fault-tolerant schemes is proved using the simulation results. In order to evaluate the performance of the proposed fault-tolerant control strategy, the simulations have been carried out on the PSIM platform for a grid connected wind power generation system. The parameters for a PMSG, grid voltage, and current are given in the Table 1. An open-switch fault S_1 is introduced at t=0.2 sec in the upper switch of a-phase of the GSC as shown in Figure 3. The faulty condition is created by turning OFF the gate signals of the corresponding switches.

Table 1. Parameters of a PMSG, grid voltage, and current

Rated power	5 kW
Rated speed	300 rpm
Number of poles	24
Flux linkages	0.36 Wb
Torque	156 Nm
Stator resistance	0.64 Ω
Stator inductance	0.82 mH
Grid voltage	359.2 V
Grid current	29.2 A

To detect the fault, the normalized three-phase grid RMS currents are used. During the normal operation, the normalized grid RMS current values become 0.5. However, when the fault occurs, three-phase normalized grid RMS currents are increased beyond the threshold values i_{th1}. Figure 6 shows the simulation results of three-phase grid currents without fault-tolerant scheme and with the proposed fault-tolerant scheme. In these figures, the term "*fault_status*" indicates the detection of fault and t_a, t_b, and t_c represents the gating signals. After the fault detection, the proposed fault-tolerant scheme is implemented at t=0.217sec. The grid currents are returned to the regular shape again within 0.0096 sec with the activation of the proposed fault-tolerant strategy as shown in Figure 6(b). When the fault occurs, the grid current waveforms diverge from their references instantly before the fault-tolerant operation. This is due to the nonlinearities introduced in the inverter topologies with the fault occurrence. This kind of phenomenon can be eliminated as soon as the fault-tolerant procedure is executed.

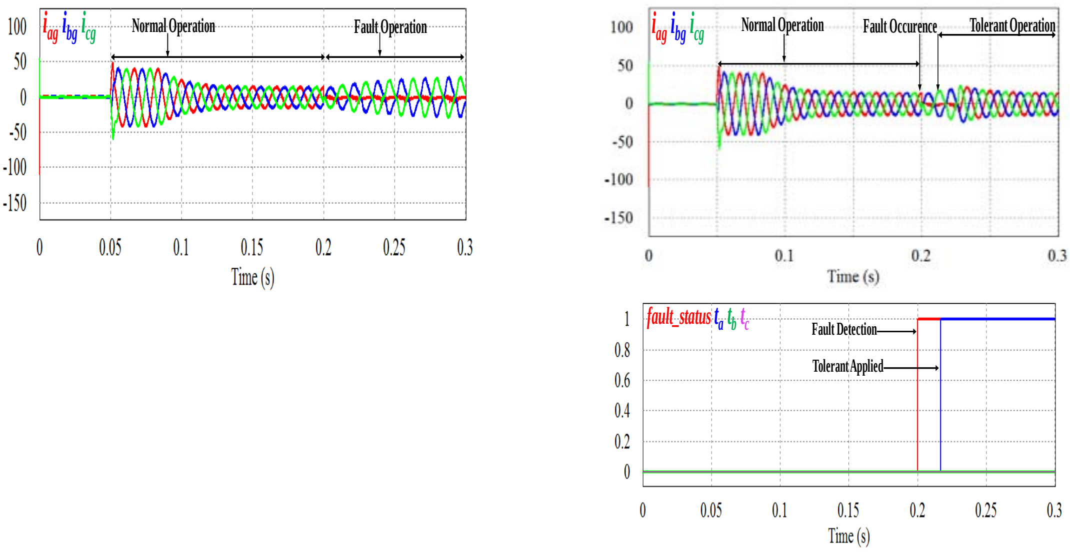

(a) Without fault-tolerant scheme (b) With fault-tolerant scheme

Figure 6. Responses of three-phase grid currents under S_1 open-switch fault

Responses of the *d*-axis and *q*-axis currents for this case are shown in Figure 7. Without fault-tolerant scheme, the *d*-axis and *q*-axis currents have big fluctuation as shown in Figure 7(a) due to S_1 open-switch fault. However, since this open-switch fault is well compensated using the proposed algorithm, the currents are stabilized within very short time as shown in Figure 7(b), once the fault-tolerant algorithm is applied.

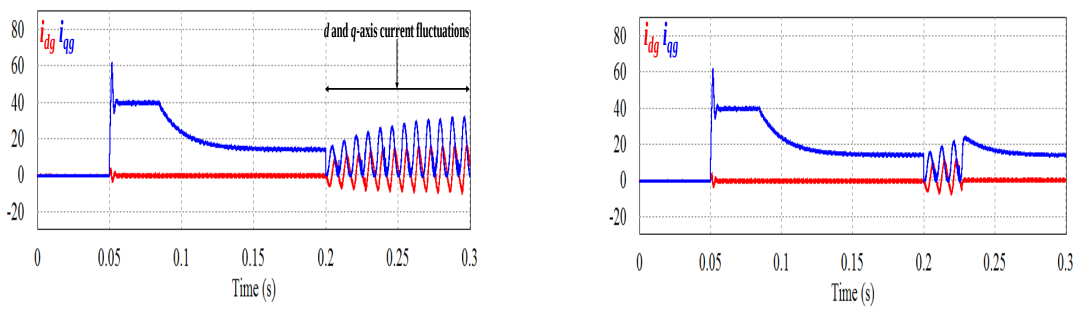

(a) Without fault-tolerant scheme (b) With fault-tolerant scheme

Figure 7. Responses of *d*-axis and *q*-axis currents under S_1 open-switch fault

Figure 8 and Figure 9 illustrate the responses of the DC link voltage and grid output power. In these figures, $V_{dc,\ ref}$ represents the DC link voltage reference and P_{out} the grid output power. During the normal operation before the fault is introduced at t=0.2 sec, the DC link voltage is well regulated and the grid output power is constant. As a result of the open-switch fault occurrence, however, the DC link voltage is increased and the grid output power is decreased gradually. With the fault-tolerant operation, the DC link voltage and grid output power reach steady-state again as like as the normal operation. After the fault detection, it is necessary to find out the faulty phase quickly to compensate the faulty phase current. If the abnormal operation lasts continuously, there is a high possibility of secondary faults in the GSC system and load. To find out the faulty phase accurately, the durations of positive and negative phase currents are used. If the open-switch fault occurs on upper switch, the corresponding phase has only the negative current because the faulty upper switch cannot conduct current as shown in Figure 6. If the open-switch fault occurs on bottom switch, the corresponding phase has only the positive current. Therefore, the fault detection and the fault-tolerant control techniques are required to make the system operation balanced. If the single open-switch fault occurs in the GSC, a faulty phase current can either be positive or negative depending on the damaged switch.

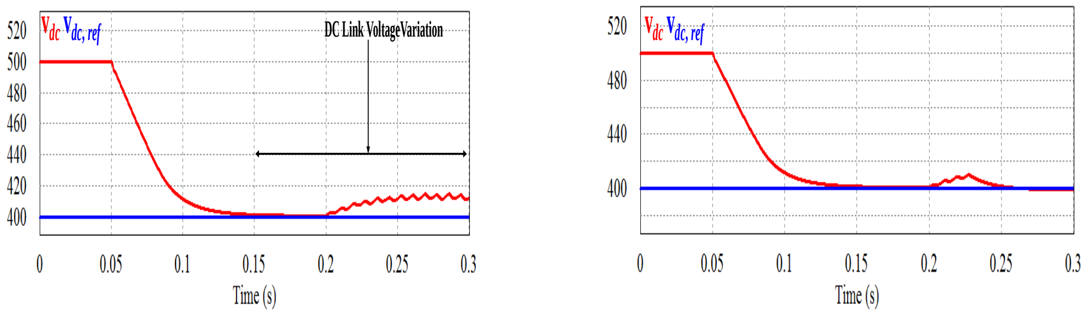

(a) Without fault-tolerant scheme (b) With fault-tolerant scheme

Figure 8. Responses of DC link voltage under S_1 open-switch fault

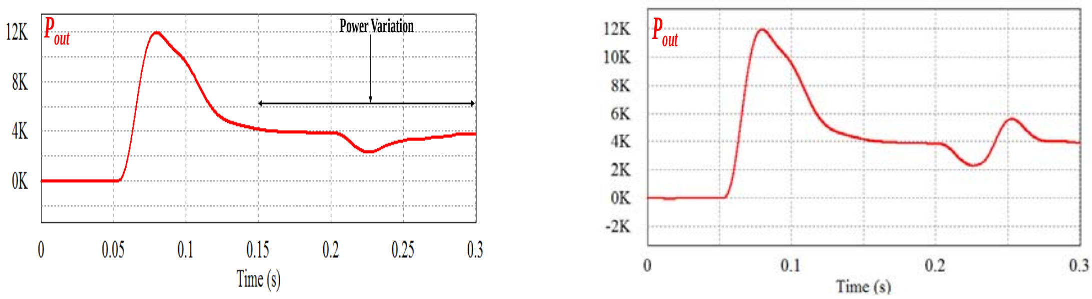

(a) Without fault-tolerant scheme (b) With fault-tolerant scheme

Figure 9. Responses of grid output power under S_1 open-switch fault

Figure 10 through Figure 13 shows the simulation results under the open-switch fault in S_1 and S_3, which is created by turning OFF the gate signals in a-phase and b-phase upper switch simultaneously. Before the fault occurs, it is well observed in these figures that the entire system provides balanced three-phase grid currents, constant regulated DC link voltage, and constant grid output power except for the short transient periods. However, when the fault is introduced into the system, phase currents are distorted as shown in Figure 10 (a). Also, as can be observed in Figure 11(a), Figure 12(a), and Figure 13(a), significant disturbance is introduced to the overall system response. The q-axis current cannot be controlled and the DC link voltage is increased sharply, which may yield a severe secondary fault in the DC link capacitor. A big drop in the grid output power is observed, which means that a proper power transfer cannot be achieved.

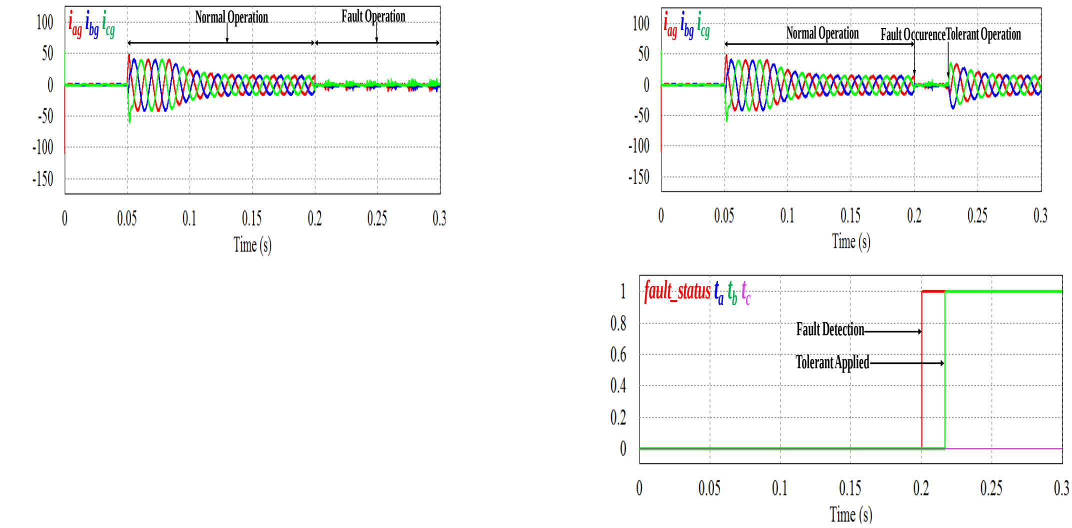

(a) Without fault-tolerant scheme (b) With fault-tolerant scheme

Figure 10. Responses of three-phase currents under S_1 and S_3 open-switch fault

On the contrary, by using the proposed scheme, the fault is detected in 0.194ms and the faulty switch is recognized in 0.0164s. Once the faulty switch is identified, the corresponding faulty phases are isolated using the TRIAC switches. To restore the system, the TRIAC switches for the corresponding redundant leg are turned ON and the gate signals for the faulty leg are transferred to the redundant leg. As a result, three-phase grid current waveforms, the *d*-axis and *q*-axis current waveforms, and the DC link voltage control performance can be recovered from the fault condition as shown in Figure 10(b) through Figure 12(b). The grid output power continues to run as the same as the pre-fault situations.

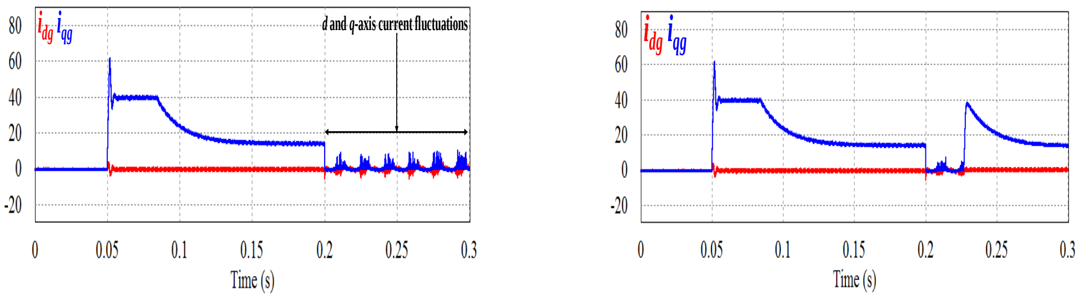

(a) Without fault-tolerant scheme (b) With fault-tolerant scheme

Figure 11. Responses of *d*-axis and *q*-axis currents under S_1 and S_3 open-switch fault

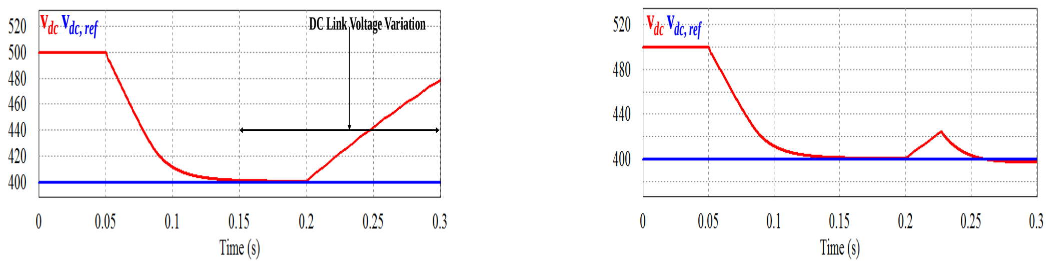

(a) Without fault-tolerant scheme (b) With fault-tolerant scheme

Figure 12. Responses of DC link voltage under S_1 and S_3 open-switch fault

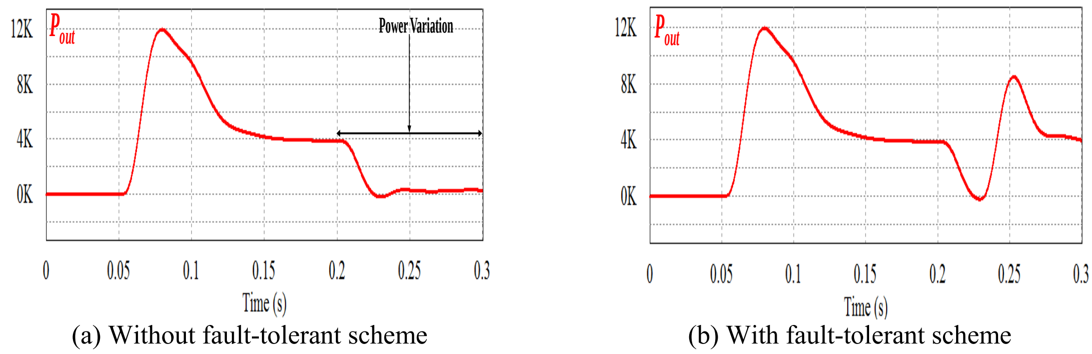

Figure 13. Responses of grid output power under S_1 and S_3 open-switch fault

5. CONCLUSION

Open-switch fault detection and fault-tolerant methods in three-phase GSC of a WECS with a PMSG have been proposed, which are able to detect and compensate the open-switch fault in single switch as well as in multiple switches. The proposed fault-tolerant topology permits the continuous operation of the GSC through a reconfiguration strategy without any false alarm. According to the position of the open-switch fault, the dramatic change in the normalized RMS currents can be observed. Normalized RMS currents are used to detect the open-switch fault. The open-switch fault detection method with the ability of fault-tolerant control makes total system much more reliable. The proposed fault compensation is achieved by reconfiguring the power converter topology with the TRIAC switches. For this purpose, additional legs are added as hardware redundancy and the TRIAC switches are used to replace the faulty leg. The proposed method is simple in construction and easy to control. Simulation results prove that the TRIAC switches can successfully isolate the faulty leg in all the fault cases. In addition, it can be confirmed from the simulation results that the proposed method can be used effectively for multiple open-switch faults. As a result, a grid connected WECS having the postfault performance with the same as the prefault case can be constructed.

ACKNOWLEDGEMENTS

This research was supported by Basic Science Research Program through the National Research Foundation of Korea (NRF) funded by the Ministry of Education (NRF-2014R1A1A2056436).

REFERENCES

[1] Ribeiro RLA, Jacobina BC. Fault-Tolerant Voltage-Fed PWM Inverter AC Motor Drive Systems. *IEEE Transactions on Industrial Electronics*. 2004; 51(2): 439-446.

[2] Ko YJ, Lee KB. Fault Diagnosis of a Voltage-Fed PWM Inverter for a Three-parallel Power Conversion System in a Wind Turbine. *Journal of Power Electronics*. 2010; 10(6): 686-693.

[3] Estima JO, Cardoso AJM. A New Algorithm for Real-time Multiple Open-Circuit Fault Diagnosis in Voltage-Fed PWM Motor Drives by the Reference Current Errors. *IEEE Transactions on Industrial Electronics*. 2013; 60(8): 3496-3505.

[4] Zidani F, Diallo D, Benbouzid MEH, Naït-Saïd R. A Fuzzy-Based Approach for the Diagnosis of Fault Modes in a Voltage-Fed PWM Inverter Induction Motor Drive. *IEEE Transactions on Industrial Electronics*. 2008; 55(2): 586-593.

[5] Farnesi S, Fazio P, Marchesoni M. *A New Fault Tolerant NPC Converter System for High Power Induction Motor Drives*. 11th Diagnostics for Electric Machines, Power Electronics & Drives (SDEMPED). Bologna 2011; 337-343.

[6] Lu B, Sharma SK. A Literature Review of IGBT Fault Diagnostic and Protection Methods for Power Inverters. *IEEE Transactions on Industry Applications*. 2009; 45(5): 1770-1777.

[7] Shahbazi M, Poure P, Saadate S, Zolghadri MR. FPGA-Based Reconfigurable Control for Fault-Tolerant Back-to-Back Converter Without Redundancy. *IEEE Transactions on Industrial Electronics*. 2013; 60(8): 3360-3371.

[8] Estima JO, Cardoso AJM. A New Approach for Real-time Multiple Open-Circuit Fault Diagnosis in Voltage-Source Inverters. *IEEE Transactions on Industry Applications*. 2011; 47(6): 2487-2494.

[9] Errabelli RR, Mutschler P. Fault-Tolerant Voltage Source Inverter for Permanent Magnet Drives. *IEEE Transactions on Power Electronics*. 2012; 27(2): 500-508.

[10] Benbouzid MEH, Diallo D, Zeraoulia M. Advanced Fault-Tolerant Control of Induction-Motor Drives for EV/HEV Traction Applications: From Conventional to Modern and Intelligent Control Techniques. *IEEE Transactions on Vehicular Technology*. 2007; 56(2): 519-528.

[11] Diallo D, Benbouzid MEH, Makouf A. A Fault-Tolerant Control Architecture for Induction Motor Drives in Automotive Applications. *IEEE Transactions on Vehicular Technology*. 2004; 53(6): 1847-1855.

[12] Song Y, Wang B. Analysis and Experimental Verification of a Fault-Tolerant HEV Powertrain. *IEEE Transactions on Power Electronics*. 2013; 28(12): 5854-5864.

[13] Parker AM, Ng C, Li R. Fault-Tolerant Control for a Modular Generator-Converter Scheme for Direct-Drive Wind Turbines. *IEEE Transactions on Industrial Electronics*. 2011; 58(1): 305-315.

[14] Flannery PS, Venkataramanan G. A Fault Tolerant Doubly Fed Induction Generator Wind Turbine Using a Parallel Grid Side Rectifier and Series Grid Side Converter. *IEEE Tranactions on Power Electronics*. 2008; 23(3): 1126-1135.

[15] Maharajan L, Yamagishi T, Hirofumi A. Fault-Tolerant Operation of a Battery-Energy-Storage System Based on a Multilevel Cascade PWM Converter With Star Configuration. *IEEE Transactions on Power Electronics*. 2010; 25(9): 2386-2396.

[16] Darly SS, Ranjan PV, Rabi BJ, Bindu KV. Fault Tolerant Control in Z-Source Inverter Fed Induction Motor. *IAES International Journal of Power Electronics and Drive System*. 2011; 1(1): 29-35.

[17] Elbarbary ZMS, Elkholy MM. Performance Analysis of Field Orientation of Induction Motor Drive under Open Gate of IGBT Fault. *IAES International Journal of Power Electronics and Drive System*. 2013; 3(3): 304-310.

BIOGRAPHIES OF AUTHORS

Partha Sarati Das was born in Chandpur, Bangladesh, in 1986. He received the M.Eng. degree in electrical and electronic engineering from Dhaka University of Engineering and Technology, Gazipur, Bangladesh, in 2012. Currently he is working toward the M.S. degree in the Department of Electrical and Information Engineering at Seoul National University of Science and Technology. His research interests include renewable energy, power electronics, wireless power transmission, VLSI circuits (analog & digital).

Kyeong-Hwa Kim was born in Seoul, Korea, in 1969. He received the B.S. degree from Hanyang University, Seoul, Korea, and the M.S. and Ph.D. degrees from Korea Advanced Institute of Science and Technology (KAIST), Taejon, Korea, in 1991, 1993, and 1998, respectively, all in electrical engineering. From 1998 to 2000, he was a Research Engineer with Samsung Electronics Company, where he was engaged in research and development of AC machine drive systems. From 2000 to 2002, he was a Research Professor with KAIST. From August 2010 to August 2011, he was a Visiting Scholar with Virginia Polytechnic Institute and State University (Virginia Tech), Virginia. Since August 2002, he has been with Seoul National University of Science and Technology, where he is currently a Professor. His current research interests are in the areas of AC machine drive, control, diagnosis, power electronics, renewable energy, and DSP-based control applications. Prof. Kim is a member of the Korean Institute of Power Electronics (KIPE) and IEEE.